Journal of Applied Electrochemistry **33**: 533–540, 2003.

Electroactive polymer films for stainless steel corrosion protection

P. HERRASTI*, P. OCÓN, A. IBÁÑEZ and E. FATÁS
*Universidad Autónoma de Madrid, Facultad de Ciencias. Dept. Química Física Aplicada 28049, Madrid, Spain (*author for correspondence, e-mail: Pilar.Herrasti@uam.es)*

Received 29 July 2002; accepted in revised form 18 February 2003

Key words: corrosion protection, microhardness, polypyrrole and polyaniline composite, potentiodynamic curves

Abstract

Electroactive polymer films of polyaniline, poly-*o*-toluidine and a composite of both were deposited on stainless steel and their performance as protective coatings against corrosion was evaluated. Open circuit potential and potentiodynamic studies of the polymer-coated stainless steel in a corrosive medium showed a significant shift in the corrosion potential towards more positive values. Mechanical characteristics of the films were evaluated by means of microhardness measurements, revealing nonelastic films in all cases and low hardness values that increased from polyaniline to poly-*o*-toluidine to the composite. The best results were obtained in the case of the polyaniline-*o*-toluidine composite.

1. Introduction

Practical applications of conductive polymers like polyaniline (Pani), polypyrrole (Ppy) and polythiophene (Pthy) have been subject to research in many fields. Protection of oxidizable metals against corrosion is one application that has been intensively investigated. Many corrosion control methods using coating and conversion films have been proposed, but all involve environmentally hazardous materials. Consequently, it is necessary to find a nontoxic replacement. Conducting polymers can be used as protective primer coatings [1–8] that can be either chemically [9–14] or electrochemically deposited [15–17]. Chemical deposition has been performed mainly with Pani and its derivatives, using *N*-methyl-2-pyrrolidinone to stabilize the emeraldine base solution. Electrochemical deposition has been performed mainly with Ppy and to a lesser extent with Pani. With the latter method, the main problems of the process are essentially related to the nature of the substrate, since each metal needs specific conditions to deposit the conducting polymer. As is well known, depending on their oxidation grade these polymers can be insulating or conductive. Insulating polymers can act as a diffusion barrier while conductive polymers confer active protection by exchanging electrons with the metallic substrate. Protection is afforded by the oxidation or passivation of the metal, shifting the corrosion potential towards more positive values and modifying the oxygen reduction reaction.

Polyaniline is one conductive polymer used for coating that has been intensively investigated. Deberry [18] found that a decrease in the corrosion rate occurred for a prepassivated steel coated with an electrochemically generated polyaniline film. In this case the polymer acts as a redox catalyst and as if it were a noble metal with respect to iron. Wessling [19] has established a general reaction mechanism, according to which polyaniline intervenes (as a redox catalyst) in the reaction between oxidizable metals and oxygen/water to form a passivating oxide layer. The proposed scheme is as follows, where EB represents emeraldine base, ES emeraldine salt and LE leucoemeraldine:

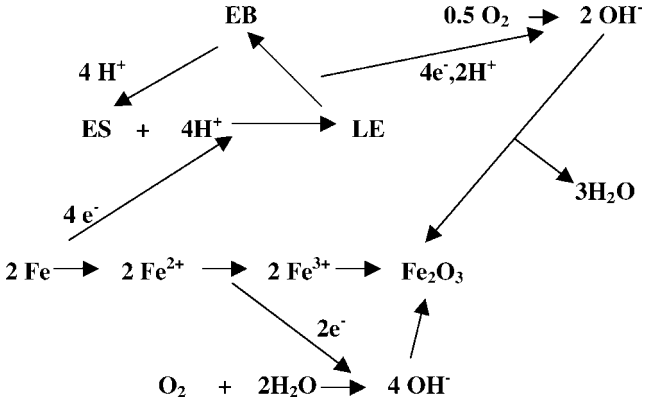

The results published hitherto in the field of corrosion protection are in many cases far from satisfying. To assure good protection, the mechanical properties of the film must also be taken into account. In general the adhesion, wear resistance and other mechanical properties of electrosynthetized polyaniline films are unsatisfactory. For technological applications, the measurement of hardness is a useful method for gauging the quality of a material. This method can be used to monitor

heat-treatment procedures on metals, to study microstructures and to examine various coatings on substrates. When hardness is measured at microscale, damage to the surface is minimal and the method can be regarded as virtually nondestructive. The measurement of macrohardness is a well known, quick and simple method of obtaining the mechanical properties of bulk materials, but where materials have a fine microstructure, are multiphase, nonhomogeneous, or prone to cracking, macrohardness measurements will be highly variable and will not identify individual surface features. It is here that microhardness measurements are appropriate.

The main objective of this work was to obtain a polymer coating able to efficiently protect stainless steel against corrosion. The general strategy was based on interfacial modification of the substrate with thin electrocatalytic films of Pani, poly-*o*-toluidine (p-*o*-tol) and a composite of the two (poly-*o*-tol-ani), either to stabilize the potential in the passive region, where the substrate is covered with oxide, or to act as a barrier between the substrate and electrolyte solution. Universal microhardness measurements were used to determine the mechanical characteristics of the three polymer coatings.

2. Experimental details

Cyclic voltammetry, potentiostatic and potentiodynamic experiments were performed in a typical single compartment three-electrode cell using a Versat-stat PAR potentiostat/galvanostat. Type 304 stainless steel foils, 1 cm^2, (0.08% C, 2% Mn, 1% Si, 18% Cr, 8% Ni) were used as working electrodes. Prior to deposition they were mechanically polished with abrasive paper, rinsed with water and acetone and air dried. A graphite plate (5 cm^2) placed parallel to the WE, was used as counter electrode and all the measurements were made against a Ag/AgCl (KCl sat.) reference electrode. The monomers (aniline and *o*-toluidine) were distilled prior to use. H_2SO_4 and NaCl were used as-received. Purified water (obtained by passing house-distilled water through a Millipore water purifying system) was used to prepare all the solutions.

To evaluate corrosion resistance, the potential was scanned from the corrosion potential to 1.2 V at a rate of 5 mV s^{-1} in 3% NaCl and 1 M H_2SO_4 solutions at room temperature. The open circuit potential was measured in a two-electrode system in both 3% NaCl and 1 M H_2SO_4 solutions using the polymer or copolymer coated stainless steel as working electrode against a Ag/AgCl (KCl sat.) reference electrode.

The surface morphology of the substrate and polymer film was studied with a Phillips XL30-EDAX PV 9900 scanning electron microscope.

For microhardness measurements a Fischerscope HV 100 tester was used. The instrument comprises a load-generating unit with a Vickers indenter. The final load applied in each case was dependent on the thickness and response of the coating, so optimum loads had to be established through several tests in order to eliminate the influence of the substrate. The testing time of the load–unload cycle was 20 s and five tests were performed along the surface to obtain a mean value.

The universal microhardness value measured with this kind of test is defined by the following formula:

$$HU = \frac{F}{26.3\ h^2}$$

where F is the load applied in each step and h is the indentation depth. Each applied load value corresponds to an indentation depth, so several values of HU are measured. For a completely homogeneous specimen one single HU value is found, while in the case of coatings on substrates with different hardness values, a change is observed in the slope of the indentation depth against square root of the applied load.

Universal microhardness testing by means of indentation depth measurement is described elsewhere [20].

3. Results and discussion

Pani and P-*o*-tol polymers can be electrodeposited on stainless steel either by potential cycling or at constant potential. The films obtained with both methods are in general homogeneous, but in some cases their adhesion is not as good as may be desired. To improve film adhesion we have attempted to copolymerize aniline and *o*-toluidine. It is well known that the polymerization rate follows the order: polyaniline > poly-*o*-toluidine > poly (*o*-toluidine + aniline) [21]. Figure 1(a) for the polymerization of 0.2 M aniline in 1 M H_2SO_4 acid shows, on the first scan at 1.1 V vs Ag/AgCl, KCl, an anodic current as a result of the oxidation of aniline, which increases with cycling. Three redox couples of polyaniline appear after five cycles. During the cathodic sweep only a single broad peak appears, and a shift in the maximum is observed with the number of cycles. By comparison with the CV of aniline in the same solution but on a platinum substrate (Figure 1(b)) it can be deduced that the peak corresponding to the polyaniline film that appears in the second cycle is due to a passive metal oxide film which is first formed on the stainless steel. Similar features are observed in the case of *o*-toluidine, though the intensity of the peaks is lower here than in the case of aniline, and fewer species are formed. This is due to the architecture of *o*-toluidine, in which the CH_3 groups can be oriented to form a barrier band on the substrate. This band prevents the attachment of new *o*-toluidine molecules to active sites on the electrode surface. With the copolymerization of aniline and *o*-toluidine, the intensity of the peaks is lower than in the case of aniline deposition. The reason, mentioned above, is that the *o*-toluidine molecules are preferentially adsorbed on the electrode surface to form a $-CH_3$ barrier, resulting in the predominance of *o*-toluidine molecules in the copolymerization. Similar results were

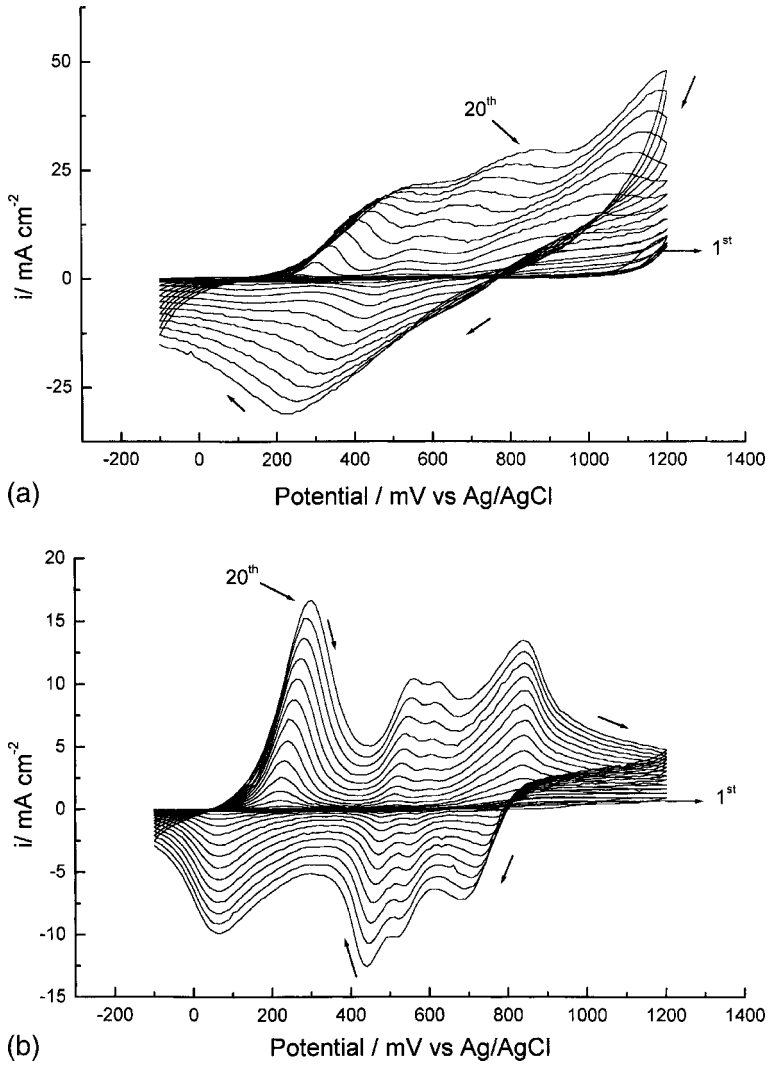

Fig. 1. (a) Voltammogram for the formation of polyaniline in 0.2 M aniline + 0.5 M H_2SO_4, at 100 mV s^{-1} on a stainless steel electrode. (b) voltammogram for electrodeposition of polyaniline on platinum substrate.

obtained by Yang [21] in the electropolymerization of toluidines on thermally prepared platinum electrodes.

Electropolymerisation at constant potential was carried out in solutions containing the monomer and 1 M H_2SO_4. The most suitable electropolymerization potential was chosen after several experiments with different potentials and electrodeposition times. It is already known that pulse potentiostatic conditions affect the early stages of the growth of Pani [22]. Thus, processes such as oligomerization, nucleation and growth are strongly dependent on the potential perturbation. Hence, different perturbation potentials during the growth of the coating lead to films containing different amounts of hydrolysis products, which also affects the morphology of the film. Chronoamperograms recorded using the best conditions for the electrodeposition of Pani are shown in Figure 2. In the procedure followed, a first pulse from 1.2 V (10 s) to 1.0 V (30 s) is applied to allow the formation of the large number of radical cations necessary for polymerization. In this anodic pulse the initial current spike was followed by a rising transient, indicating an initial process of oxidation of the steel and subsequent growth of the polymer film. A second pulse in the polyaniline polymerization was applied from 0 to 0.8 V. Application of more positive potentials is not recommended, since at potentials above 0.9 V the transpassive dissolution of stainless steel begins and the adhesion of the Pani film to the steel surface decreases. After the initial spike, the current increases due to the polymer's deposition upon the first oxide layer generated during the first pulse. Similar potentiostatic experiments were carried out for *o*-toluidine and the *o*-toluidine-aniline composite polymerization. In both cases the second pulse goes up to 1.0 V, because at lower potentials only falling transients were observed. The absence of rising transients indicates that there was no increase in the electroactive surface area of the polymer film and, therefore, little or no polymer growth.

3.1. *Corrosion behaviour*

Corrosion of metals involves the transfer of electrical charge in aqueous solutions at the metal–electrolyte interface. Corrosion protection is often afforded by

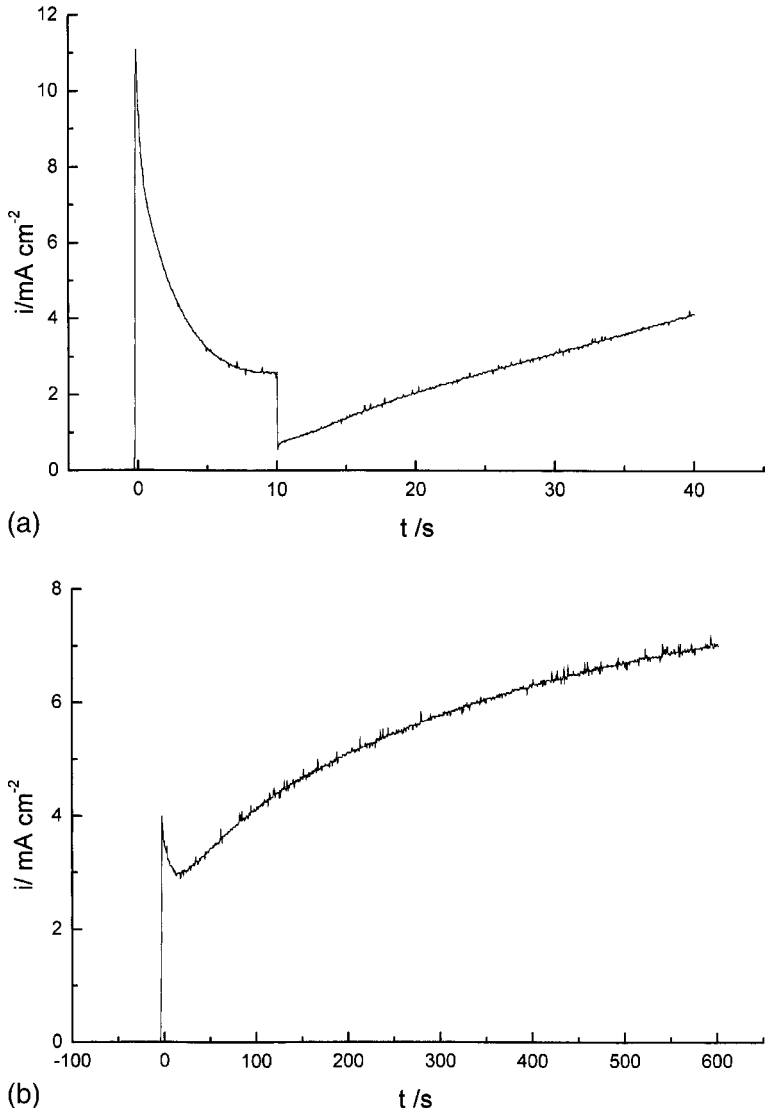

Fig. 2. Chronoamperometric response of stainless steel in 0.2 M aniline + 0.5 M H_2SO_4. First transient (a) was the response to the pulse from 1.2 V (10 s) to 1.0 V (30 s) and second transient (b) was obtained at 0.8 V.

isolating metals from the corrosive environment using polymer coatings. These polymer films need to have good barrier properties and to remain adherent in the presence of corrosive products such as strong acid media or NaCl solutions.

Electrochemical measurements (corrosion potential against time and corrosion current) and scanning electron microscopy at different stages have been used to assess the protective properties of the coating in the supporting electrolytes. Figure 3 shows the corresponding open circuit potential (V_{corr}) against time curves in 1 M H_2SO_4. When bare stainless steel is exposed to this solution, the initial V_{corr} of −200 mV soon rises up to 150 mV and after 11 days has dropped to a steady state value of −200 mV. By comparison, when a Pani-coated film is immersed in 1 M H_2SO_4 solution, the V_{corr} is initially equal to 250 mV but decreases until $V_{corr} = -200$ mV, that is, the same value as bare stainless steel, which indicates that the film is not very protective. This film was obtained by cyclic voltammetry, stopping the

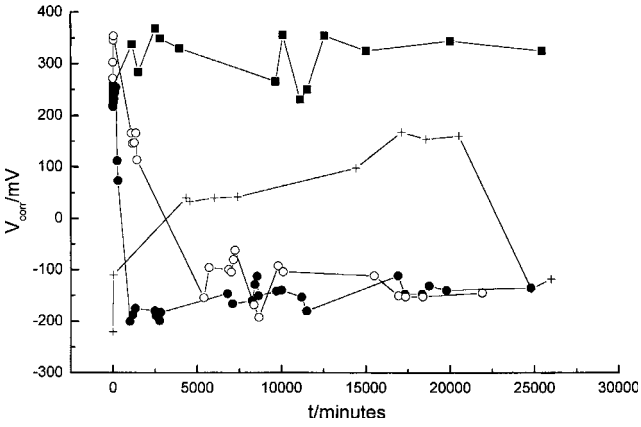

Fig. 3. Plots of open circuit potential against time in 1 M H_2SO_4 solution of (+) bare stainless steel electrode, (○) poly-*o*-tol coated steel electrode, (●) Pani coated steel electrode and (■) composite coated steel electrode. Polymers were obtained by cyclic voltammetry.

potential at a reduction value. Considering that the redox potential of polyaniline depends on the $(Pani)_{ox}$/

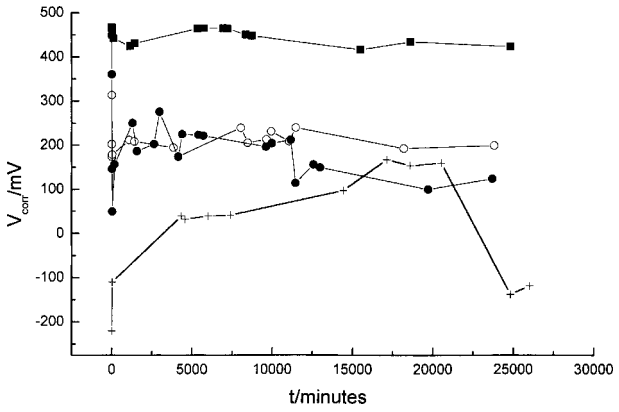

Fig. 4. Plots of open circuit potential against time in the same conditions as Figure 3, but in this case the polymers were obtained at constant potential.

$(Pani)_{red}$ concentration ratio, the low potential values obtained imply the existence of more Pani in reduced state than in oxidised state. With regard to the cathodic reaction of the corrosion process, from a thermodynamic point of view, protons cannot oxidize Pani if the potential is in the range of 0.2 to −0.18 V vs Ag/AgCl because the equilibrium potential for the H^+/H_2 system is −0.22 V vs Ag/AgCl. Dissolved oxygen (from the air) cannot be the oxidizing agent because its amount is not enough to oxidize polyaniline by increasing the corrosion potential. When bare steel is coated with P-*o*-tol the V_{corr} against time curve is similar, and when it is coated with the P-*o*-tol + Pani composite the V_{corr} remains at about 300 mV for a longer time. In the latter case the composite is probably used as a cement and cross-linker, preventing the entry of protons and other ions, and consequently enhancing corrosion protection. All the measurements have demonstrated that the electrodeposition of composite films yields better performance than single Pani or P-*o*-tol films. This can be seen in Figure 4 when the film has been obtained at constant potential. In this case the concentration of oxidized species produced the persistence of a constant positive corrosion potential V_{corr}.

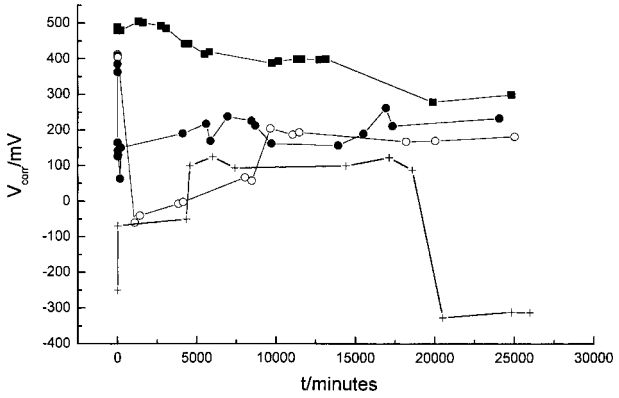

Fig. 5. Plots of open circuit potential against time with the same polymers obtained at constant potential in 3% NaCl.

The curve obtained in a medium containing 3% NaCl is shown in Figure 5 for a film deposited at constant potential. The general characteristics are similar to the case of the H_2SO_4 medium, but here the V_{corr} potential remains for a longer time at a higher value due to the deprotonation induced by the 3% NaCl solution. The species formed are stabler and the redox potential of the film corresponds to that of the passive region. In essence the Fermi level of the underlying metal is shifted to and maintained at more positive values.

3.2. *Potentiodynamic polarization*

Figure 6 shows the potentiodynamic polarization curves of bare stainless steel and steel coated, respectively, with Pani, P-*o*-tol and the composite. The corresponding corrosion potentials (V_{corr}) and corrosion currents (i_{corr}) are listed in Table 1. The corrosion potential shifts from a more negative value, corresponding to bare stainless steel, to a more positive value (370 mV); showing an inhibition of the corrosion process by the polymer coating. In contrast, the corrosion current density rises from 1.9×10^{-6} to 1.12×10^{-3} A cm^{-2}, which seems to be in contradiction with the values of V_{corr}. The increase in the corrosion current could be due to several factors and not only to the oxidation of metal (e.g., doping of the polymer), oxidation of the film and/or insertion of anions as counter ions in the polymer structure. This behaviour has been reported previously [23–25]. To check this affirmation we have applied a potential of 0.6 V to stainless steel coated with the composite in a

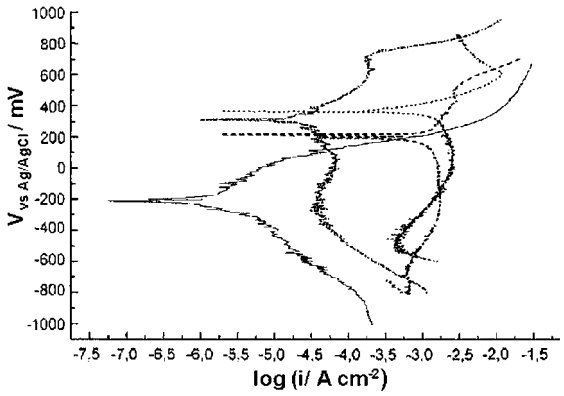

Fig. 6. Tafel plots at 10 mV s^{-1} in 3% NaCl solution of (——) bare stainless steel electrode, (- - - -) Pani coated steel electrode, (-·-·-·) poly-*o*-tol coated steel electrode and (···) poly-*o*-tol-ani coated steel electrode.

Table 1. Corrosion parameters for bare steel and steel coated with different polymers

Substrate	V_{corr} /mV	i_{corr} /A cm^{-2}
Stainless	−225	1.9×10^{-6}
Pani	200	1.12×10^{-3}
P-*o*-tol	300	4.51×10^{-5}
P-*o*-tol-ani	370	1.25×10^{-3}

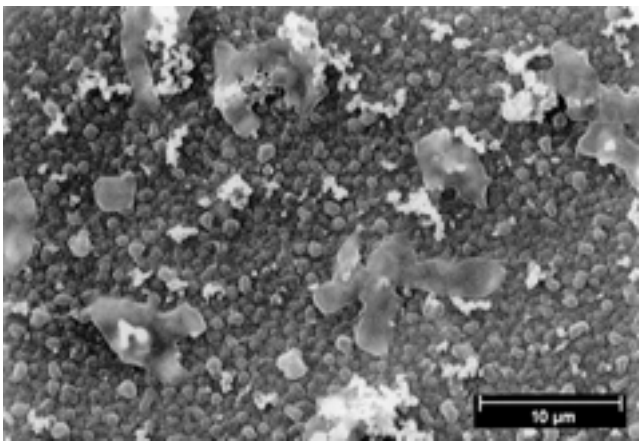

Fig. 7. Micrograph of polyaniline before treatment.

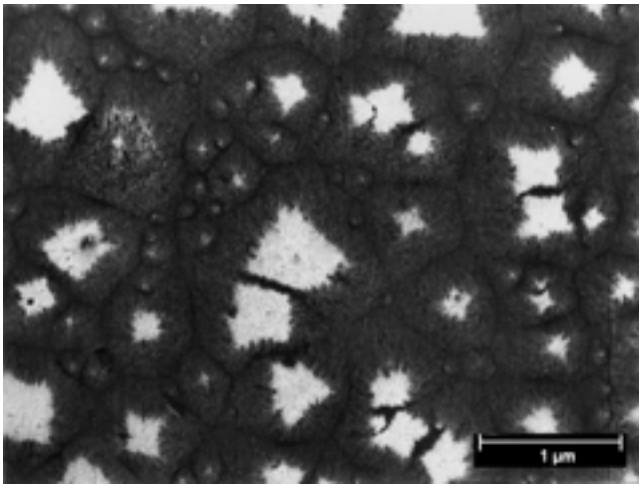

Fig. 8. Micrograph of polyaniline after 15 days in 1 M H_2SO_4 solution.

3% NaCl solution for 120 s. When the polymer is scratched the surface of the stainless steel does not show a pitting pattern. If the potential applied is higher than 0.9 V, the surface of the stainless steel after scratching the polymer reveals a typical pitting pattern produced by the attack of chloride ions. This suggests that the current observed in the polarization curves at low potentials corresponds to oxidation of the polymer, and also explains why this current, which is not strictly a corrosion current, is higher than the corrosion current density in the case of stainless steel.

3.3. *Microstructure*

Figure 7 shows a micrograph of a polyaniline film before being immersed in the aggressive medium. Its morphology is globular and is very similar to the film obtained on a platinum substrate.

Figure 8 shows a SEM image of a polyaniline film after 15 days in 1 M H_2SO_4. Cracks are observed across the surface of the film, allowing the electrolyte solution to access the underlying stainless steel. Lighter, more

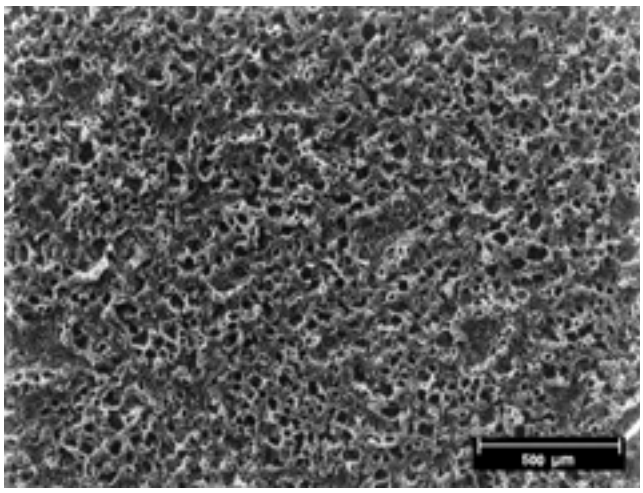

Fig. 9. Micrograph of poly-*o*-toluidine after 15 days in 1 M H_2SO_4.

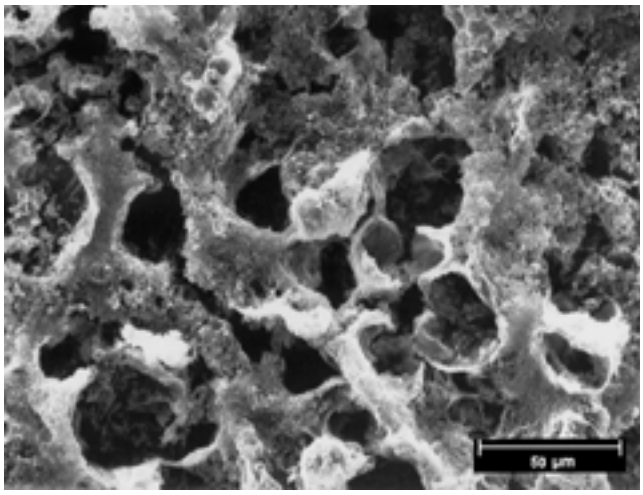

Fig. 10. Same sample as Figure 9 at greater magnification.

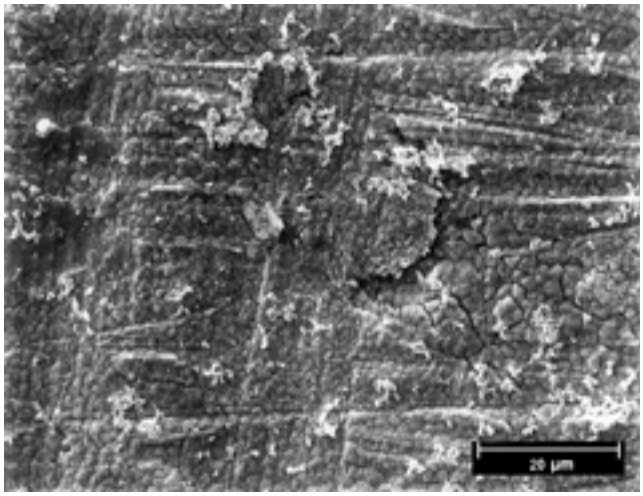

Fig. 11. Micrograph of the composite grown at constant potential after 15 days in 1 M H_2SO_4 solution.

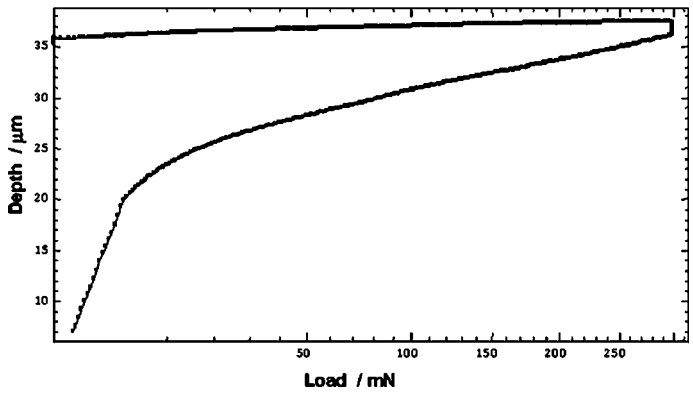

Fig. 12. Indentation depth as a function of the applied test load for the composite.

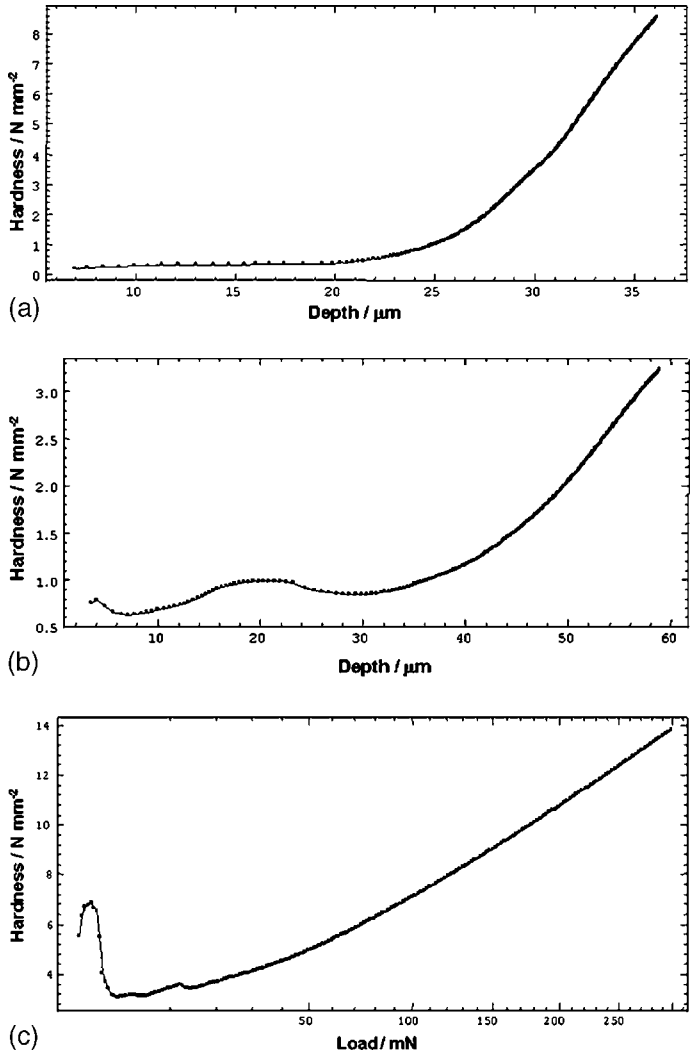

Fig. 13. Microhardness as a function of indentation depth for (a) Pani, (b) P-*o*-tol and (c) composite.

attacked zones are observed on the surface. These areas correspond to points with more irregularities, where the polymer is more easily degraded.

Figures 9 and 10 show two micrographs of poly-*o*-toluidine also after 15 days in 1 M H_2SO_4. Both samples present holes across the surface that can be more clearly appreciated in Figure 10. Inside the holes the polymer continues to cover the stainless steel surface. Figure 11 displays a micrograph of the Poly-*o*-tol-ani composite growth at constant potential. No cracks or holes are observed after 15 days in H_2SO_4, indicating again that the composite renders good corrosion protection.

3.4. *Hardness testing*

Plots of indentation depth against the square root of the applied load, for both increasing and decreasing test cycle load phases, are shown in Figure 12. It can be seen how the indentation depth increases steeply up to 23 μm, after which the increase in the slope is more gradual, due to the influence of the substrate's greater hardness. Figure 13 shows the hardness of three films, (a) Pani, (b) P-*o*-tol and (c) the composite against indentation depth. As can be observed, hardness is low and increases in the order Pani < P-*o*-tol < composite. Hardness values correspond to the initial linear part of the plot. In all cases these values remain constant up to about 20 μm, which is the estimated thickness of the film. It can also be seen that the constant value of hardness with indentation depth in the case of Pani (Figure 13(a)) indicates a homogeneous character of this film, while the variation observed with P-*o*-tol corresponds to an inhomogeneous response in depth of this coating. In the case of the composite a surface layer of a few microns is slightly harder and the bulk is quite homogeneous.

The curve of indentation depth vs. applied load can be used to evaluate elastic recovery. Figure 12 indicates that the composite presents no elastic recovery. The same tendency is found for the other two polymer films.

4. Conclusions

A composite film was prepared by electrosynthesis from a solution containing aniline and *o*-toluidine monomers. This composite film presents better corrosion protection than that conferred by Pani or P-*o*-tol alone. Protection in an aggressive medium of 1 M H_2SO_4 or 3% NaCl is effective for at least 30 days. If a low current is passed through the steel coated with the composite, the steel is still protected from the aggressive medium, as is shown by polarisation experiments. Hardness has been measured for the three polymer films and the best mechanical properties have been found in the case of the composite.

Acknowledgements

The authors would like to thank CICYT (Spain) for financial support under project no. BQU2001-0149. We also express our gratitude to Centro de Tratamiento de Superficies, C.T.S. for allowing the use of microhardness measuring equipment.

References

1. A. Meneguzzi, M.C. Pham, J.C. Lacroix, B. Piro, A. Adenier, C.A. Ferreira and P.C. Lacaze, *J. Electrochem. Soc.* **148** (2001) B121.
2. J.L. Camalet, J.C. Lacroix, S. Aeiyach, K. Chane-Ching and P.C. Lacaze, *Synth. Met.* **93** (1998) 133.
3. T. Zalewska, A. Lisowska-Oleksiak, S. Biallozor and V. Jasulaitiene, *Electrochim. Acta* **45** (2000) 4031.
4. C.W. Yan, H.C. Lin and C.N. Cao, *Electrochim. Acta* **45** (2000) 2815.
5. J.O. Iroh and W. Su, *Electrochim. Acta* **46** (2000) 15.
6. S. Aeiyach, B. Zaid and P.C. Lacaze, *Electrochim. Acta* **44** (1999) 2889.
7. M.A. Malik, M.t. Galkowski, H. Bala, B. Grzybowska and P.J. Kulesza, *Electrochim. Acta* **44** (1999) 2157.
8. T. Dung Nguyen, J.L. Camalet, J.C. Lacroix, S. Aeiyach, M.C. Pham and P.C. Lacaze, *Synth. Met.* **102** (2000) 1388.
9. B. Wessling and J. Posdorfer, *Electrochim. Acta* **44** (1999) 2139.
10. R. Gasparac and C.R. Martin, *J. Electrochem. Soc.* **148** (2001) 13138.
11. N. Ahmad and A.G. MacDiarmid, *Synthetic Metals* **78** (1996) 103.
12. B. Wessling, *Synth. Met.* **93** (1998) 143.
13. S.R. Morais, D. Huerta-Vilca and A.J. Motheo, *Mol. Cryst. Liq. Cryst. Sci. Technol., Section A* **374** (2002) 391.
14. L.H.C. Mattoso, S.K. Manohar, A.G. MacDiarmid and A.J. Epstein, *J. Polym. Sci. A*; *Polym. Chem.* **33** (1995) 127.
15. J.O. Iroh and W. Su, *Electrochim. Acta.* **46** (2000) 15.
16. B. Zaid, S. Aeiyach and P.C. Lacaze, *Synth. Met.* **65** (1994) 27.
17. G. Troch-Nagels, R. Winand, A. Weymeersch and L. Renard, *J. Appl. Electrochem.* **22** (1992) 756.
18. D.W. DeBerry, *J. Electrochem. Soc.* **132** (1985) 1022.
19. B. Wessling, *Mater. Corros.* **47** (1996) 439.
20. W. Weiler, *Br. J. Non-Destr. Test.* **31** (1989) 253.
21. C.-H. Yang, *J. Electroanal. Chem.* **459** (1998) 71.
22. G. de T. Andrade, M.J. Aguirre and S.R. Biaggio, *Electrochim. Acta* **44** (1998) 633.
23. J.R. Santos, L.H.C. Mattoso and A.J. Motheo, *Electrochim. Acta* **43** (1998) 309.
24. P. Herrasti and P. Ocón, *Appl. Surf. Sci.* **172** (2001) 276.
25. L.F. D'Elia, R.L. Ortiz, O.P. Marquez, J. Marquez and Y. Martínez, *J. Electrochem. Soc.* **148** (2001) C297.